An H_2 Optimal Adaptive Power System Stabilizer

Antal Soós, Om P. Malik

Abstract— **Application of an H_2 optimal adaptive control algorithm as power system stabilizer is described in this paper. The algorithm deals with disturbance attenuation in the sense of H_2 norm for non-linear systems. Results of simulation and experimental studies suggest that the H_2 optimal control algorithm could be successfully used for the control of non-linear systems such as synchronous generators.**

Keywords— **adaptive control, optimal control, power systems.**

I. Introduction

A power system is a sophisticated combination of multiple electrical and mechanical components. In general, these elements are non-linear and their parameters vary with operating conditions, random load changes and unpredictable disturbances. These characteristics present a challenge for control algorithm design.

Control of non-linear systems has received substantial attention in recent years [1],[2]. Although many analytical techniques and design methodologies have been developed, comparatively few studies [3],[4],[5] present the H_2 or H_∞ non-linear control applications due to the lack of efficient numerical methods for solving the required optimization problems. In these studies the structure of the plant is restricted to a minimal structure needed to show the relevant mathematical aspects of the solution. The question of how these methods can be applied to solve engineering problems remains unaddressed.

An alternative solution to this non-linear control problem is presented in this paper, where the non-linear variable parameter plant is approximated with a linear variable parameter adaptive model. In the adaptive algorithm the parameters of the linearized model are continuously estimated at the operating point of the plant. From the robustness point of view, the adaptive control is used to reduce the uncertainty level of the plant model by using an appropriate plant model identifier in closed-loop operation [6].

Application of the proposed adaptive controller as a power system stabilizer is described. The adaptive-control design technique is based on an explicit identification of the linearized transfer function of the plant in real time. A modified recursive least squares algorithm (RLS), that increases the robustness of the identification algorithm during large disturbances, is used for parameter identification. The optimal control is calculated by solving on-line algebraic Riccati equation for the identified closed-loop system model obtained by the RLS identification algorithm. States of the system required for control computation are estimated with an adaptive Kalman Filter. The control is calculated each sampling interval on-line.

The proposed optimal adaptive power system stabilizer (OAPSS) is free from repetitive parameter tuning required with the fixed parameter conventional power system stabilizer (CPSS), a lead-lag network. Comparative studies show that the proposed OAPSS exhibits better performance than the CPSS.

Financial support of NSERC Canada is acknowledged for this work.

A. Soós, TyCom (US) Inc., Eatontown, NJ. E-mail: asoos@ieee.org
O.P. Malik, Professor Emeritus, The University of Calgary, E-mail: malik@enel.ucalgary.ca

II. Optimal controller structure

A. System parameter estimation

All techniques for analysis and design of control systems are based on the availability of appropriate models for the process dynamics. The model structures are derived from the prior knowledge of the process and the disturbances. In some cases, only a priori knowledge is available so that the process can be described as a linear system in a particular operating range. It is then natural to use the general representation of linear systems, the so called black-box model [7]. A typical example is the difference-equation model in prediction form [8]:

$$y(n) = \sum_{i=1}^{m} b_i u(n-i) - \sum_{i=1}^{m} a_i y(n-i) + e_r(n) \qquad (1)$$

where $u(n)$ is the input and $y(n)$ is the output of the plant, and $e_r(n)$ is the error in the model, the so called prediction error, at sampling period n. The a_i and b_i parameters, as well as the order of the model m, are considered as unknown [9]. The model order should be determined based on the simulation and experimental studies. The a_i and b_i parameters should be determined in such a way that the cost function for the exponentially weighted error squared is minimum:

$$J_r = \sum_{i=0}^{n} \lambda^{n-i} [e_r(i)]^2 \qquad (2)$$

where λ is the forgetting factor, $0 \ll \lambda < 1$ [10]. Minimization of the cost function (2) leads to the RLS adaptive algorithm (denoted by index $_r$) [10].

The RLS algorithm presented in the literature [10] is based on the assumption that the external disturbances affecting the plant have normal (or Gaussian) distribution $N(0, \sigma^2)$, in which case the RLS algorithm optimally estimates the plant's linearized-model parameters. However, in most of the industrial systems, specifically in power systems this assumption is rarely true. Power system operation is characterized by a wide range of operating conditions, random load changes and various unpredictable disturbances. Therefore, two modifications in the RLS algorithm are introduced to achieve better performance even

in situations where the basic assumption of the normal distribution of the disturbances is violated. The first modification is in the form of a variable forgetting factor, and the second modification entails the implementation of a tracking constrained coefficient.

The use of a forgetting factor is intended to assure that data points in the distant past are "forgotten" in order to afford the possibility of following the statistical variations of the observable data when the adaptation operates in a non-stationary environment [11]. The relation between the forgetting factor λ and the memory length l measured in samples can be approximated as [9]:

$$\lambda = e^{-1/l} \tag{3}$$

where e is the base of the natural logarithm. If the forgetting factor is approaching 1 the memory length is approaching infinity, which is beneficial when the plant's operating condition is not changing, because this will ensure less variations in the estimated parameters. However, if the plant operating condition changes, the forgetting factor close to 1 will delay the estimation of the new system parameters until the new statistical values become dominant in the calculation. But, if the forgetting factor is less than 1, the estimation will be much faster. To achieve a compromise, a variable forgetting factor, $\lambda(n)$, is introduced as a function of the prediction error:

$$\lambda \ : \quad \lambda(n) = \begin{cases} \lambda_d \lambda(n-1) + (1-\lambda_d) & if \quad e_r^2(n) \le e_{trs} \\ \\ \lambda_0 & if \quad e_r^2(n) > e_{trs} \end{cases} \tag{4}$$

where e_{trs}, λ_d and λ_0 are experimentally selected pozitive constants. The threshold e_{trs} is much larger than the prediction error during steady plant operation. If the prediction error $e_r^2(n)$ exceeds e_{trs}, the forgetting factor is changed to the value $\lambda_0 < 1$, which will enable faster correction in the estimated parameters. However, if the plant is working under steady-state operating conditions, the forgetting factor will approach 1, $\lambda(n) \to 1$, resulting in less variations in the estimated parameters. The speed of this convergence is determined by the parameter λ_d.

It is a direct consequence of the least squares formulation that a single large error will have a dramatic effect on the results because the error is squared in the criterion [9]. To make the RLS algorithm more robust for major disturbances, the tracking constrained coefficient, $\beta(n)$, is introduced in the algorithm:

$$\beta(n) = \begin{cases} 1 & if \quad N_2/N_1 \le \beta_0 \\ \\ \beta_0/N_2 & if \quad N_2/N_1 > \beta_0 \end{cases} \tag{5}$$

where

$$N_1(n) = \| \ \mathbf{\Theta}(n-1) \ \|_2, \qquad N_2(n) = \| \ \mathbf{K}_r(n) e_r(n) \ \|_2 \tag{6}$$

The β_0 parameter is an empirically selected threshold to detect the presence of large disturbances. The $\mathbf{K}_r(n)$ and $\mathbf{\Theta}(n-1)$ variables are the gain vector (9) and parameter vector (8), respectively, defined in the RLS algorithm below. The tracking constrained coefficient used during the estimate update calculation, in (7), works as an inhibitor. If the prediction error $e_r(n)$ deviates from the normal distribution, the tracking constrained coefficient will eliminate this effect on the parameter update calculation by taking a much smaller value $\beta(n) = \beta_0/N_2$ than the increase in the $e_r(n)$ prediction error. During the period when the plant is working in an environment with normally distributed disturbances, this mechanism will not have any effect on the parameter estimation because the tracking constrained coefficient will take a neutral value $\beta(n) = 1$.

The RLS algorithm [10], modified as above, is presented below:

$$\mathbf{\Theta}(n) = \mathbf{\Theta}(n-1) + \mathbf{K}_r(n) e_r(n) \beta(n) \tag{7}$$

$$\mathbf{\Theta}(n) = [b_1(n) \cdots b_m(n), a_1(n) \ldots a_m(n)]^T \tag{8}$$

$$\mathbf{K}_r(n) = \frac{\mathbf{P}_r(n-1)\Psi(n)}{\lambda(n) + \mathbf{\Psi}^T(n)\mathbf{P}_r(n-1)\mathbf{\Psi}(n)} \tag{9}$$

$$\mathbf{\Psi}(n)^T = [u(n-1) \cdots u(n-m), y(n-1) \cdots y(n-m)] \tag{10}$$

$$\mathbf{P}_r(n) = \frac{\mathbf{P}_r(n-1) - \mathbf{K}_r(n)\mathbf{\Psi}^T(n)\mathbf{P}_r(n-1)}{\lambda(n).} \tag{11}$$

$$e_r(n) = y(n) - \mathbf{\Psi}^T(n)\mathbf{\Theta}(n-1) \tag{12}$$

B. State space representation

So far the plant parameter $\mathbf{\Theta}(n)$ estimation has been described, which is based on the difference-equation representation (1). In the following, the matrix state-space representation will be used. Specifically, the transformation from difference equation to state space equation is shown in this section. Based on the estimated system parameters, the dynamic system in state-space representation can be described by the process (13) and measurement (14) equation:

$$\mathbf{x}(n+1) = \mathbf{A}(n)\mathbf{x}(n) + \mathbf{B}(n)u(n) + \mathbf{G}w(n) \tag{13}$$

$$\hat{y}_k(n) = \mathbf{C}\mathbf{x}(n) + v(n) \tag{14}$$

where:

$$\mathbf{A}(n) = \begin{bmatrix} -a_1 & 1 & 0 & \cdots & 0 \\ -a_2 & 0 & 1 & \ddots & \vdots \\ -a_3 & \vdots & \ddots & \ddots & 0 \\ \vdots & & & \ddots & 1 \\ -a_m & 0 & \cdots & & 0 \end{bmatrix}, \mathbf{B}(n) = \begin{bmatrix} b_1 \\ b_2 \\ \vdots \\ b_m \end{bmatrix} \tag{15}$$

$$\mathbf{G} = [1, 1 \cdots 1]^T, \quad \mathbf{C} = [1, 0 \cdots 0] \tag{16}$$

and $w(n)$ and $v(n)$ in (13) and (14) represent the modeling inaccuracies and the measurement noise, respectively.

With the state-space representation a new variable $\mathbf{x}(n)$, the so called state-space vector (13), has emerged. This vector represents the internal state of the plant, which can be best estimated with Kalman Filter. The Kalman Filter

(denoted by index $_k$), for the plant state estimation, is based on a cost function minimization process [12] :

$$J_k(n) = E[v^2(n)] \tag{17}$$

For the Kalman Filter implementation it is necessary to assume that $w(n)$ and $v(n)$ are white noise processes with zero mean, and covariance is defined by [13] :

$$E\{w(k)w(i)\} = \begin{cases} Q_k(k) & i = k \\ 0 & i \neq k \end{cases} \tag{18}$$

$$E\{v(k)v(i)\} = \begin{cases} R_k(k) & i = k \\ 0 & i \neq k \end{cases} \tag{19}$$

where $E\{\circ\}$ is the statistical expectation.

The role of these two covariances in the Kalman Filter is to adjust the Kalman gain in such a way that it controls the filter "bandwidth" as the state and the measurement error vary [14]. In practice, this information is usually not known totally, and in previous Kalman Filter implementations these values were estimated based on a priori measurements. In the OAPSS algorithm, the covariances are estimated by using a curve-fitting method, which eliminates the need for a priori studies.

The prediction error $v(n)$ in the Kalman Filter is the difference between the plant's output $y(n)$ and predicted output $\hat{y}_k(n) = \mathbf{C}\mathbf{x}(n)$. The source of the prediction error $v(n)$ is the unmodeled system dynamics - the noise measured on the system output. The conventional estimate for the covariance of this noise, $R_k(n)$, can be calculated using the N most recent prediction errors $v(n)$ see equation (22), as presented in [15].

$$v(n) = y(n) - \mathbf{C}\mathbf{x}(n-1) \tag{20}$$

$$\overline{v} = \frac{1}{N}\sum_{i=1}^{N} v(n-i) \tag{21}$$

$$R_k(n) = \frac{1}{N-1}\sum_{i=1}^{N} [v(n-i) - \overline{v}]^2 \tag{22}$$

Prediction error $e_r(n)$ of the RLS algorithm for system parameter estimation and process noise in the Kalman Filter $w(n)$ represent the same characteristics of the model - the error in the model parameters. Using this parallelism, the prediction error $e_r(n)$ of the RLS adaptive algorithm can be used as an "estimate" of the error in the system model $w(n)$ [16]. The estimate of the state noise covariance can be calculated using (24).

$$\overline{e}_r = \frac{1}{N}\sum_{i=1}^{N} e_r(n-i) \tag{23}$$

$$Q_k(n) = \frac{1}{N-1}\sum_{i=1}^{N} [e_r(n-i) - \overline{e}_r]^2 \tag{24}$$

The Kalman Filter algorithm [10] is presented below:

$$\mathbf{P}_k^-(n) = \mathbf{A}(n)\mathbf{P}_k(n-1)\mathbf{A}^T(n) + \mathbf{G}Q_k(n)\mathbf{G}^T \tag{25}$$

$$\mathbf{x}^-(n) = \mathbf{A}(n)\mathbf{x}(n-1) + \mathbf{B}(n)u(n-1) \tag{26}$$

$$\mathbf{K}_k(n) = \frac{\mathbf{P}_k^-(n)\mathbf{C}^T}{\mathbf{C}\mathbf{P}_k^-(n)\mathbf{C}^T + R_k(n)} \tag{27}$$

$$\mathbf{P}_k(n) = \mathbf{P}_k^-(n) - \mathbf{K}_k(n)\mathbf{C}\mathbf{P}_k^-(n) \tag{28}$$

$$\mathbf{x}(n) = \mathbf{x}^-(n) + \mathbf{K}_k(n)[y(n) - \mathbf{C}\mathbf{x}^-(n)] \tag{29}$$

C. Optimal control calculation

The optimal control (denoted by index $_c$) is computed by using the identified model parameters and estimated states of the system. Based on linear control theory [17], the quadratic performance index used in the finite-horizon H_2 control is defined as:

$$J_c(n) = \sum_{k=0}^{N} \mathbf{x}^T(n-k)\mathbf{Q}_c\mathbf{x}(n-k) + u^T(n-k)R_c u(n-k) \tag{30}$$

where N is finite, $\mathbf{Q}_c$ is symmetric positive semi-definite and R_c is positive. The control signal calculation, with the input output decoupling noise for adaptive algorithm, is shown below:

$$u(n) = -\mathbf{K}_c(n)\mathbf{x}(n) + RMS(n) \tag{31}$$

where $RMS(n)$ is a random multilevel sequence, scaled to the required noise level for the adaptive algorithm. The optimal control algorithm is [17]:

$$\mathbf{K}_c(n) = \frac{\mathbf{B}^T(n)\mathbf{P}_c(n-1)\mathbf{A}(n)}{\mathbf{B}^T(n)\mathbf{P}_c(n-1)\mathbf{B}(n) + R_c} \tag{32}$$

$$\mathbf{P}_c(n) = \mathbf{A}^T\mathbf{P}_c(n-1)[\mathbf{A}(n) - \mathbf{B}(n)\mathbf{K}_c(n)] + \mathbf{Q}_c \tag{33}$$

The final selection of $\mathbf{Q}_c$ and R_c is based on repeatedly varying q_i and r_1 parameters (34). In a rudimentary way, it can be expected that increase in q_i will result in a reductin of system state error, while increase in r_1 will lead to a control effort reduction. By varying these parameters the desired control characteristics are achieved. For initial guess [18] [19]:

$$\mathbf{P}_c(0) = \mathbf{Q}_c = diag(q_1 \cdots q_m), \quad R_c = r_1 \tag{34}$$

where $\mathbf{Q}_c$ is a $m \times m$ matrix and R_c is scalar. The resulting control algorithm is shown in Fig. 1.

D. Initialization

The forgetting factor $\lambda(0) = \lambda_0$ for the adaptive algorithm, where λ_0 $(= 0.98)$ is the reset value and λ_d $(= 0.998)$ is the time constant for adaptive forgetting factor. The threshold for error e_{trs} and tracking constrained coefficient β_0 should be selected such that in steady-state operation $e_{trs} > e_r^2(n)$, $\beta_0 > N_2/N_1$, and during the exogenous disturbances $e_{trs} < e_r^2(n)$, $\beta_0 < N_2/N_1$. During the initial adaptation, while the algorithm starts with zero system parameter, $\Theta(0) = [0, 0 \cdots 0]^T$, the tracking constrained coefficient function should be disabled, $\beta(n) = 1$, until the prediction error achieves its steady value. Otherwise, the

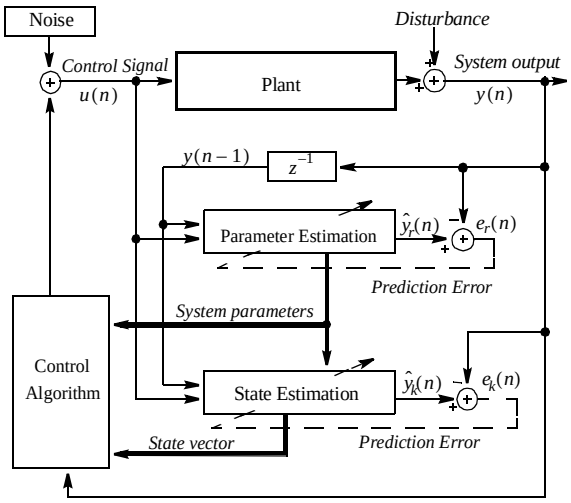

Fig. 1. Adaptive Optimal Control Structure

system parameter identification will be prohibited by the constraint function.

Initial values for the RLS algorithm and Kalman Filter recursion can be seleced based on the equations (35-37) and (38-39) respectively.

$$\mathbf{\Theta}(0)^T = [0 \cdots 0], \quad 1 \times 2m \tag{35}$$

$$\mathbf{\Psi}(0)^T = [0 \cdots 0], \quad 1 \times 2m \tag{36}$$

$$\mathbf{P}_r(0) = \delta \mathbf{I}^{2m \times 2m} \tag{37}$$

where $\mathbf{I}^{2m \times 2m}$ is a $2m \times 2m$ unity matrix, and δ $(= 10^{12})$ is a large constant.

$$\mathbf{x}(0)^T = [0 \cdots 0], \quad 1 \times m \tag{38}$$

$$\mathbf{P}_k(0) = 0.01 \mathbf{I}^{m \times m}. \tag{39}$$

III. Simulation studies

The plant used in this study is a synchronous generator connected to a constant voltage bus through a double-circuit long transmission line. A continuously acting Automatic Voltage Regulator (AVR) is added to the excitation system. The power system model and the parameters are described in [21], [22]. Based on the experiments, it was concluded that the model order less than three is inadequate and the model order more than five does not show significant improvement. Therefore,the model order m $(= 3 \; or \; 5)$ is selected according to the system's physical behavior [20]. The OAPSS takes inputs from the error in speed (deviation in the generator speed) signal. The power system with the proposed controller is shown in Fig. 2. The results are compared with those of the conventional IEEE Standard 421.5, Type ST1A AVR and Exciter Model and an IEEE Standard 421.5, PSS1A Type CPSS [23].

A. Voltage reference step change

With the generator operating at a power of 0.7 pu, 0.99 pf lag, a very large (10%) step increase in the reference voltage was applied. The system response with the CPSS and OAPSS under this condition is shown in Fig. 3.

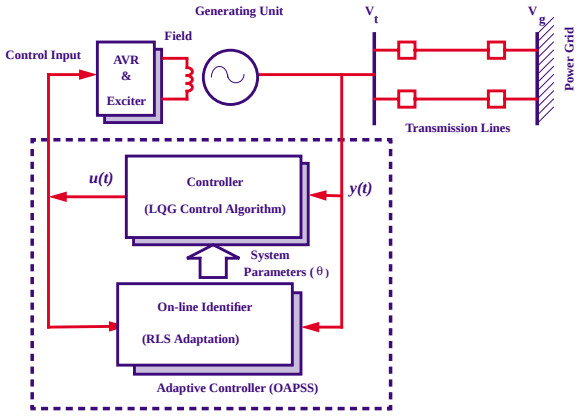

Fig. 2. Simulation studies

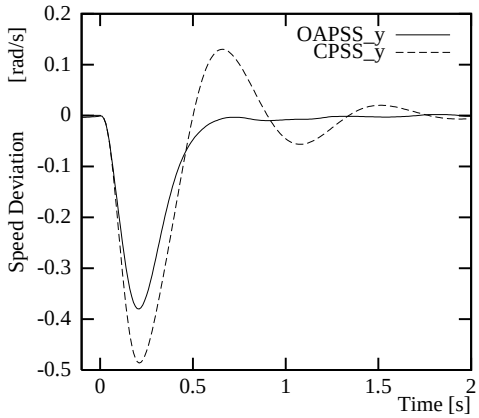

Fig. 3. Reference voltage 10% increase, P=0.7 pu, 0.99 pf lag

B. Input torque reference step change

With the generator operating at a power of 0.2 pu, with 0.85 pf lag, a 40% step increase in input torque reference was applied. The system response, Fig. 4a, and the control actions with the CPSS and OAPSS controllers are shown in Fig. 4b.

C. Voltage reference step change

With the generator operating at a power of 0.3 pu, 0.85 pf lead, a 10% step decrease in the reference voltage was applied. The system response with CPSS and OAPSS under this condition is shown in Fig. 5.

D. Fault test

To verify the behavior of the proposed adaptive algorithm under extreme conditions, a 3 phase to ground short was applied at the middle of one transmission line and cleared 100 ms later by the disconnection of the faulted line. The response is shown in Figs. 6. For this test, the operating conditions of the generator were set to 0.7 pu, 0.62 pf lag.

IV. Experimental tests

The behavior of the proposed OAPSS has been further investigated on a physical model of a single machine con-

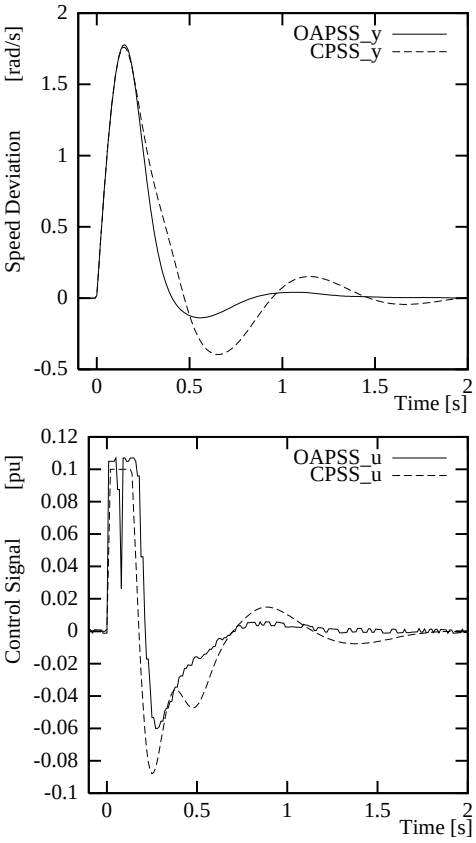

Fig. 4. Speed deviation and control for 0.4 pu mechanical power reference step change, P=0.2 pu, 0.85 pf lag

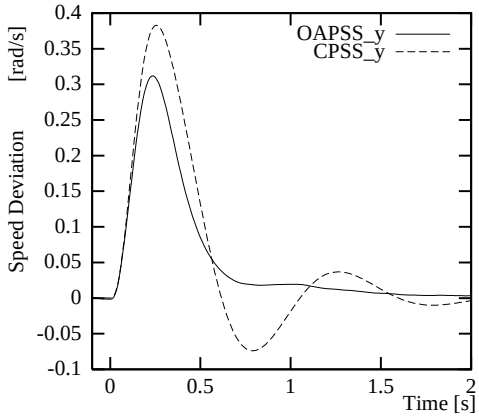

Fig. 5. 0.1 pu voltage reference step decrease P=0.3 pu, 0.85 pf lead

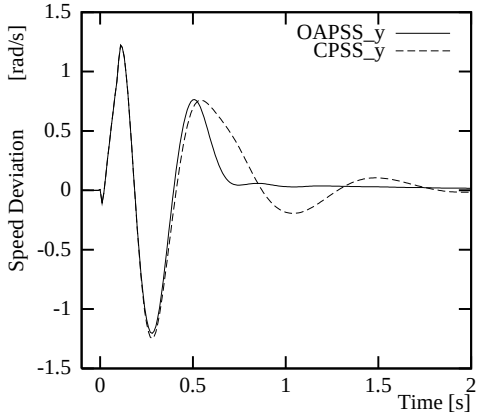

Fig. 6. 3 phase to ground fault, P=0.7 pu, 0.62 pf lag

stant voltage bus power system under various operating conditions and disturbances. Compared to the simulation studies, where the speed deviation signal was observed as a system indicator, in experimental tests the power output was used in the control loop. The major reason for this is that for experimental work the power output is more readily available. Also, the changes in power output and the changes in speed are related.

The model is available in the Power System Research Laboratory at the University of Calgary. It consists of a 3-phase 3 kVA micro-synchronous generator connected to a constant voltage bus through a double circuit transmission line model. The transmission lines are modeled by six π sections. The lines had parameters equivalent to 300 km of 500 kV line. The field time constant of the generator was adjusted to a value typical of a large machine by using a time-constant regulator [24]. An overall schematic diagram of this physical model is given in Fig. 7. The major units of this model are: the turbine *M*, the generator *G*, the transmission line model and the *AVR*. The *AVR* is the *PHSC2* Programmable Logic Controller (PLC) designed for power system control by ABB of Switzerland.

The control algorithm is implemented on a single board computer, which uses a Texas Instruments TMS320C31 digital signal processor (DSP) to provide the necessary computational power. The DSP board is installed in a personal computer with the corresponding development software and debugging application program. The analog to digital input channel of DSP board receives the signal, sampled at a 50 ms interval and calculates the control signal which is converted by the digital to analog converter. The calculation time of the OAPSS is less than 37 ms. The results are compared with those of the IEEE type PSS1A CPSS, implemented on the same DSP, with a 1 ms sampling period.

A. Voltage reference step change

In this experiment the micro-synchronous generator was operated at 0.82 pu power, 0.85 pf lag. A 10% step increase in the reference voltage was applied at 0.5 s and removed at 4 s. The generator's electrical power output with the OAPSS and with the CPSS is shown in Fig. 8. It can be observed that the CPSS controller damps very slowly, oscillations lasting for 3 s before dying out, as compared to the proposed OAPSS controller. This response can be seen after 0.5 s and 4 s corresponding to the voltage input step changes. The proposed controller exhibits a faster and more controlled damping.

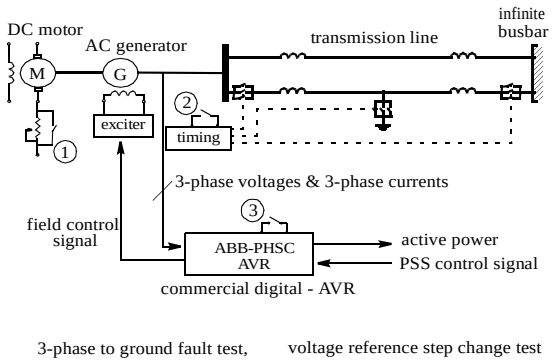

Fig. 7. Laboratory power system model

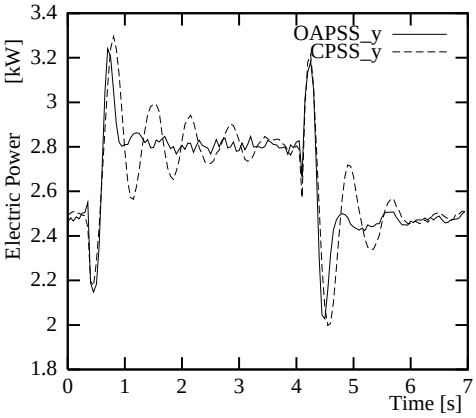

Fig. 8. OAPSS and CPSS responses for 10% voltage reference step change

B. Input torque reference step change

In this experiment the generator was operated at 0.9 pu power (2.7 kW), 0.85 pf lag. A 40% step decrease (to 1.5 kW) in the input torque was applied at 0.5 s and removed at 4.5 s. The generator electrical power with the OAPSS and with the CPSS is shown in Fig. 9. When the generator's condition changes to a lower operating point at 0.5 s both control algorithms provide good damping. However, when a 40% electric power step increase is applied to the system at 4.5 s, the system's stability margin has decreased due to the higher operating point and the performance with the OAPSS is considerably better.

C. Three-phase to ground fault test

To investigate the performance of the OAPSS under transient conditions caused by transmission line fault, a three phase to ground fault test has been conducted. In this experiment the generator was operated at 0.9 pu power (2.7 kW), 0.85 pf lag. At this operating condition, with both lines in operation, a three phase to ground fault was applied at 0.5 s in the middle of one transmission line. The faulty transmission line was opened by relay action at both ends 100 ms later. The first unsuccessful reclosure attempt was made after 600 ms, and the line was opened again 100 ms later due to a permanent fault. The second successful reclosure attempt was applied at 5 s and the system returned to the initial operating conditions. System response with the OAPSS and the CPSS under the above transient conditions is shown in Fig. 10. It can be observed that the OAPSS outperforms the CPSS with a smaller overshoot and faster settling time in both cases, at 0.5 s and 5 s.

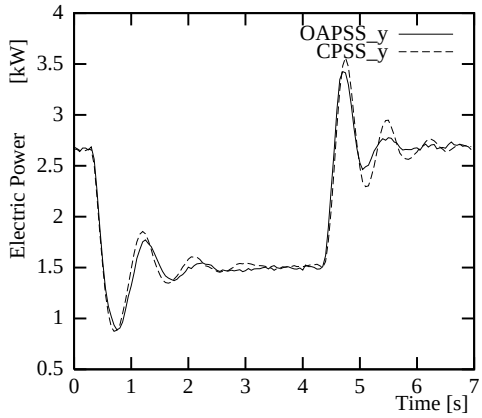

Fig. 9. Comparison of OAPSS and CPSS responses for input torque reference step change

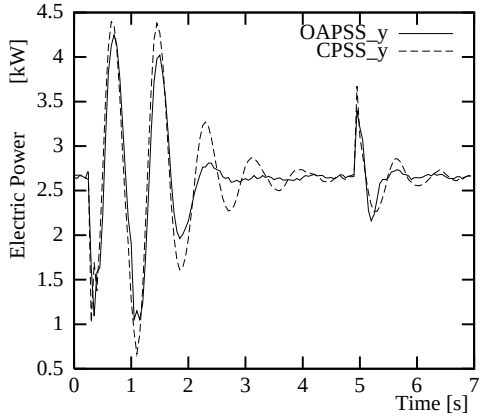

Fig. 10. Comparison of OAPSS and CPSS response for a three-phase to ground fault test

Fig. 11a presents the comparison of the performances in response to a three phase fault with the generator operating at 0.5 pu power, 0.9 pf lead. One can observe that at 2 s the system response with the CPSS shows smaller oscillations, but these oscillations increase with time and push the system into loss of synchronization until 14 s, at which time the second transmission line is restored. The system never lost synchronization with OAPSS. This test was repeated several times with the same outcome. This test demonstrated that when the system operating point significantly differs from the operating point at which the CPSS has been tuned, the system response with the OAPSS is stable but with the CPSS is unstable. The comparison of the control signals for OAPSS and CPSS is given in Fig. 11b.

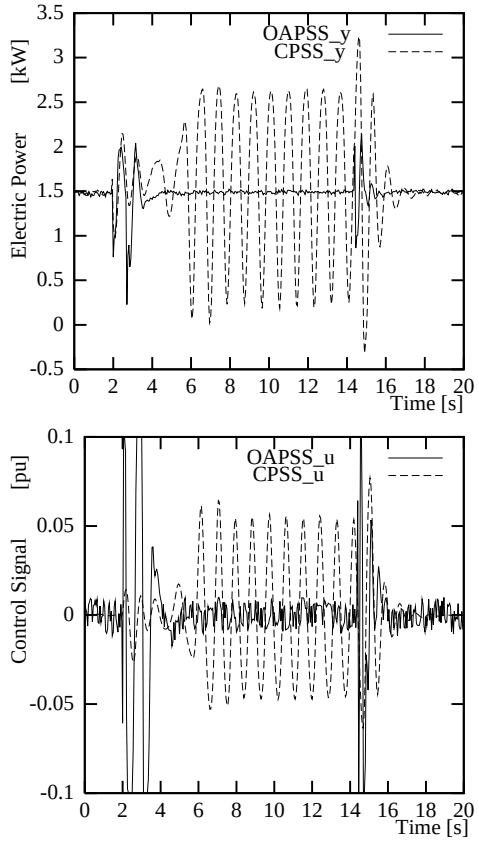

Fig. 11. Electric power and control conparison of OAPSS and CPSS responses for a three-phase to ground fault test at a leading power factor condition

V. Conclusions

The optimal control algorithm discussed in this paper has a self-tuning property. Also, the introduction of the tracking constrained coefficient increases the robustness of parameter estimation. Its application as a power system stabilizer to damp oscillations of a non-linear device, such as a synchronous generator, is illustrated by both simulation and experimental studies. Test results show that the proposed OAPSS can provide good damping over a wide operating range and improve the dynamic performance and robustness of the power system by damping the oscillations quickly even for large disturbances.

Once the parameters, which define the characteristics of control, are selected in simulation studies the control is calculated based on the estimated parameters for the existing system configuration and actual plant operating conditions. Because of this,the control algoritm does not require repetitive off-line parameter tuning. It thus provides better performance in damping the power system oscillations and will significantly reduce the cost of maintenance. Next stage in the development of the OAPSS is to illustrate its performance in the multi-machine power system environment with multi-modal oscillations.

.

References

[1] Henson M.A. & Seborg D.E., *Nonlinear Process Control*, Prentice-Hall, NJ., 1997.

[2] Helton J.W. & James R.M., *Extending H_∞ Control to Nonlinear Systems*, SIAM, Philadelphia, 1999.

[3] Beard, R., *Improving the Closed-Loop Performance of Nonlinear Systems*, PhD dissertation, Rensselaer Polytechnic Institute, Troy, NY., 1995.

[4] Christen, U. & Cirillo, R., "Nonlinear H_∞ Control - Derivation and Implementation," *Institut fur Mess- und Regeltechnik, IMRT Report*, vol. 1, no. 31, July 1997.

[5] Tsiotras, P. & Corless, M. & Rotea, M.A., "An L_2 Disturbance attenuation solution to the nonlinear benchmark problem," *International Control of Robust and Nonlinear Control*, vol. 8, no. 4, pp. 311–330, Apr. 1998.

[6] Landau, I.D., "From robust control to adaptive control," *Control Engineering Practice*, vol. 7, no. 7, pp. 1113–1124, Jul 1999.

[7] Ljung, Lennart, *System Identification Theory for the User*, Prentice-Hall, NJ., 1999.

[8] Goodwin, C.G. & Sin, K.S., *Adaptive Filtering Prediction and Control*, Prentice Hall, NJ., 1984.

[9] Astrom, K.J. & Wittenmark, B., *Computer Controlled Systems*, Prentice Hall, NJ., 1984.

[10] Haykin, S., *Adaptive Filter Theory*, Prentice-Hall, NJ., 1996.

[11] Astrom, K.J. & Wittenmark, B., *Adaptive Control*, Addison-Wesley Publishing Company, Reading, MA., 1995.

[12] Phillips, C.L. & Nagle, Jr. H.T., *Control System Analysis and Design*, Prentice-Hall, NJ., 1991.

[13] Grewal, M.S. & Andrews, A.P., *Kalman Filtering Theory and Practice*, Prentice Hall, NJ., 1993.

[14] Xia, Q. & Rao, M. & Ying, Y. & Shen, X., "Adaptive fading Kalman Filter with an Application," *Automatica*, vol. 30, no. 8, pp. 1333–1339, Aug. 1994.

[15] Moghaddamjoo, A. & Kirlin, R.L., "Robust adaptive Kalman filtering with unknown inputs," *IEEE Transaction on Acustics, Speech and Signal Processing*, vol. 37, no. 8, pp. 1166–1175, 1989.

[16] Soos, A., *An Optimal Adaptive Power System Stabilizer*, U. of C., MSc. Thesis, Calgary, October 1997.

[17] Lewis, F.L., *Applied Optimal Control & Estimation - Digital Design & Implementation*, Prentice-Hall, NJ., 1992.

[18] Bryshon, A.E. & Ho, Jr.Yu-Chi, *Applied Optimal Control*, Hemisphere Publishing Company, Washington D.C., 1975.

[19] Lin, Ching-Fang, *Advanced Control System Design*, Prentice-Hall, NJ., 1994.

[20] G.S. Hope, Malik, O.P. and M.A.H. Sheirah, "Digital implementation and test results of a self-tuning speed regulator," *Canadian-Electrical-Engineering-Journal*, vol. 6, no. 1, pp. 9–15, 1981.

[21] Ramakrishna, G. & Malik, O.P., "Adaptive control of power systems using radial basis function network identification," *1999 IEEE Power Engineering Society Summer Meeting*, vol. PES-2, pp. 989–994, July 1999.

[22] Shamsollahi, P. & Malik, O.P., "Direct neural adaptive control applied to synchronous generator," *Energy Conversion, IEEE Transactions on*, vol. 14 Issue: 4, pp. 1341–1346, 1999.

[23] IEEE Standard, *IEEE Recomanded Practice for Excitation Systems for Power System Stability Studies*, IEEE, NY., 1992.

[24] Hammons, T.J. & Parson, A.J., "Design of micro-alternator for power system- stability investigations," *Proc. IEE*, vol. 118, no. 10, pp. 1421–1439, 1971.

Antal Soós received his Dipl.Ing. degree from the University of Neoplantensis in 1986, and the MSc. degree in 1997, at the University of Calgary, both in electrical engineering. Presently, he is working towards his PhD degree. He is a member of the senior technical staff at TyCom (US) Inc.

Om P. Malik (M'66-SM'69-F'87) graduated in electrical engineering in 1952 and received the Ph.D. degree and D.I.C. in 1965. He became professor at the University of Calgary in 1974 and is presently a faculty professor. He has collaborated in research work with teams from Russia, Ukraine, China and India. In addition to his research and teaching, he has served in many additional capacities including Associate Dean (Academics/Student Affairs) and Acting Dean of the Faculty of Engineering.